DIAMOND, R. (1966). *Acta Cryst.* **21**, 253–266.
DIAMOND, R. (1971). *Acta Cryst.* A**27**, 436–452.
DODSON, E. J., ISAACS, N. W. & ROLLETT, J. S. (1976). *Acta Cryst.* A**32**, 311–315.
DUNFIELD, L. G., BURGESS, A. W. & SCHERAGA, H. A. (1978). *J. Phys. Chem.* **82**, 2609–2616.
EPP, O., COLMAN, P., FEHLHAMMER, H., BODE, W., SCHIFFER, M., HUBER, R. & PALM, W. (1974). *Eur. J. Biochem.* **45**, 513–524.
FERRO, D. R. & HERMANS, J. (1977). *Acta Cryst.* A**33**, 345–347.
FITZWATER, S. & SCHERAGA, H. A. (1980). In preparation.
GŌ, N. & SCHERAGA, H. A. (1970). *Macromolecules*, **3**, 178–187.
HERMANS, J. JR & MCQUEEN, J. E. JR (1974). *Acta Cryst.* A**30**, 730–739.
HUBER, R., KUKLA, D., BODE, W., SCHWAGER, P., BARTELS, K., DEISENHOFER, J. & STEIGEMANN, W. (1974). *J. Mol. Biol.* **89**, 73–101.
HUBER, R., KUKLA, D., RUHLMANN, A., EPP, O. & FORMANEK, H. (1970). *Naturwissenschaften*, **57**, 389–392.
JACK, A. (1977). *Acta Cryst.* A**33**, 497–499.
NYBURG, S. C. (1974). *Acta Cryst.* B**30**, 251–253.
PATTERSON, A. L. (1959). *International Tables for X-ray Crystallography*, Vol. II, p. 63. Birmingham: Kynoch Press.
PINCUS, M. R. & SCHERAGA, H. A. (1979). *Macromolecules.* **12**, 633–644.
PINCUS, M. R., ZIMMERMAN, S. S. & SCHERAGA, H. A. (1976). *Proc. Natl Acad. Sci. USA*, **73**, 4261–4265.
PINCUS, M. R., ZIMMERMAN, S. S. & SCHERAGA, H. A. (1977). *Proc. Natl Acad. Sci. USA*, **74**, 2629–2633.
PLATZER, K. E. B., MOMANY, F. A. & SCHERAGA, H. A. (1972). *Int. J. Pept. Protein Res.* **4**, 201–219.
POWELL, M. J. D. (1970*a*). *A Hybrid Method for Nonlinear Equations*, in *Numerical Methods for Nonlinear Algebraic Equations*, edited by P. RABINOWITZ, pp. 87–114. London: Gordon & Breach.
POWELL, M. J. D. (1970*b*). *A Fortran Subroutine for Solving Systems of Nonlinear Algebraic Equations*, in *Numerical Methods for Nonlinear Algebraic Equations*, edited by P. RABINOWITZ, pp. 115–161. London: Gordon & Breach.
POWELL, M. J. D. (1970*c*). *A Fortran Subroutine for Unconstrained Minimization, Requiring First Derivatives of the Objective Function*, UK At. Energy Auth., Res. Group, Culham Lab., Rep. AERE-R 6469, Harwell, England.
POWELL, M. J. D. (1970*d*). *A New Algorithm for Unconstrained Optimization*, in *Nonlinear Programming*, edited by J. B. ROSEN, O. L. MANGASARIAN & K. RITTER, pp. 31–65. New York: Academic Press.
RASSE, D., WARME, P. K. & SCHERAGA, H. A. (1974). *Proc. Natl Acad. Sci. USA*, **71**, 3736–3740.
STEIGEMANN, W. (1976). Personal communication.
SUSSMAN, J. L., HOLBROOK, S. R., CHURCH, G. M. & KIM, S. H. (1977). *Acta Cryst.* A**33**, 800–804.
SWENSON, M. K., BURGESS, A. W. & SCHERAGA, H. A. (1978). In *Frontiers in Physico-Chemical Biology*, edited by B. PULLMAN, pp. 115–142. New York: Academic Press.
TEN EYCK, L. F., WEAVER, L. H. & MATTHEWS, B. W. (1976). *Acta Cryst.* A**32**, 349–350.
WARME, P. K., GŌ, N. & SCHERAGA, H. A. (1972). *J. Comput. Phys.* **9**, 303–317.
WASER, J. (1963). *Acta Cryst.* **16**, 1091–1094.
WILLIAMS, D. E. (1972). *Acta Cryst.* A**28**, 629–635.

Acta Cryst. (1980). A**36**, 219–228

The Space-Group Determination of GaS and $Cu_3As_2S_3I$ by Convergent-Beam Electron Diffraction

BY P. GOODMAN AND H. J. WHITFIELD

CSIRO Division of Chemical Physics, PO Box 160, *Clayton, Victoria, Australia* 3168

(*Received* 1 *May* 1979; *accepted* 24 *September* 1979)

Abstract

Space-group determinations were carried out on GaS and $Cu_3As_2S_3I$ single crystals using convergent-beam electron diffraction data. The space groups found were $P6_3/mmc$ and *Cmcm*, respectively. The effectiveness of the specific test for centrosymmetry was examined. In both structures the test was made clearer by use of the inclined-axis technique, in which the incident beam is at an appreciable angle to the principal zone axis. It was concluded that the test was superior to optical methods in structures such as GaS which have a high dislocation density.

Introduction

Since the publication of a space-group identification procedure consisting of specific symmetry tests in convergent-beam electron diffraction (Goodman, 1975), a number of substances have been examined in

0567-7394/80/020219-10$01.00

this and in other laboratories (*e.g.* Tanaka, 1978), with a view to assessing its value in a practical situation. Sometimes the problem, at the stage of electron-diffraction analysis, is something less than a complete determination and involves testing for a particular symmetry element in order to distinguish between two or three possible space groups. These are problems commonly left over from an X-ray analysis. The most urgent of these problems would appear to be the determination of centrosymmetry. The direct test for centrosymmetry has therefore been examined in some detail since there has previously been some doubt as to its practicability (Goodman, 1975). Also, there has been recent interest in the effectiveness of this test relative to the optical detection of 'harmonic generation' (see for example Dougherty & Kurtz, 1976).

At the same time, it is still desirable to be able to approach a structure about which little or nothing is known, or assumed, and to arrive at a unique solution for the space group. From the examples given below it is evident that this can be achieved. In the case of GaS the conclusions are in agreement with the early X-ray determination (Hahn & Frank, 1955), although the present attempt to make this determination more accurate appeared to be worthwhile, considering that subsequent studies have shown a high susceptibility to disorder. Furthermore, it is hoped that this structure is sufficiently complex (and the unit cell sufficiently large) so that detailed observations made here will provide a working guide to the general procedure. The second study provides an example in which the identification of symmetry class and centricity by electron diffraction forced a revision of the initial symmetry assignment, which had been based on a simple interpretation of X-ray intensities, and allowed the total X-ray-plus-electron data to be correctly interpreted. This situation must be expected to arise commonly in the case of structures with moderately large unit cells.

Space-group determination of GaS

GaS crystals were prepared by reacting gallium and sulphur in stoichiometric proportions in an evacuated silica ampoule at 1173 K. Single crystals were cleaved mechanically, after glueing them individually to a grid. They contained a relatively high dislocation density but, as reported earlier (Basinsky, Dove & Mooser, 1961), these appeared to be complete dislocations and not partial ones. No sign of stacking faulting was found, and the patterns taken with the beam focused midway between dislocations indicated a very high degree of crystalline perfection.

The patterns are described in the same sequence in which they were taken. A more compact procedure could be given starting from the principal zone axis (as is done in § 3), but this assumes prior knowledge. The more detailed analysis gives a realistic working procedure for an unknown structure, since it includes identification of the major axis.

The crystal goniometer was made reasonably horizontal, and a set of (low-order) reflexions was then searched for in the vicinity of this setting. A set of strong Kossel lines was found (later indexed as the $hh\bar{2}h0$ set), and the crystal rotated about the perpendicular, $[11\bar{2}0]$, zone axis in an arbitrarily chosen sense, until a zone axis was reached. Typically, a zone axis appears over the horizon of the field of view as a dense converging set of lines inclined to the original set. This zone was pseudo-hexagonal in geometry and it was at first thought to be the main [0001] zone. The zone pattern (*E* in Fig. 1) in fact has a symmetry of only $1m$, with one mirror line through the whole pattern (Fig. 2). This result permits only one symmetry deduction, namely the existence of a vertical mirror plane.

Further rotation of the crystal in the same direction, away from the pseudo-hexagonal zone, produced a new zone pattern of rectangular geometry (*F* in Fig. 1). This zone also had a total $1m$ symmetry (Fig. 3*a*). This feature, together with a lack of inversion symmetry in the central, 0000, disc, as with the previous zone, is sufficient evidence for a vertical three-dimensional mirror plane in the structure, *i.e.* for a mirror plane containing the $[hh\bar{2}h0]$ vector and *parallel* to the incident beam. The existence of a horizontal twofold axis in the structure is demonstrated by the presence, in all satisfied reflexions of the original $hh\bar{2}h0$ set, of an

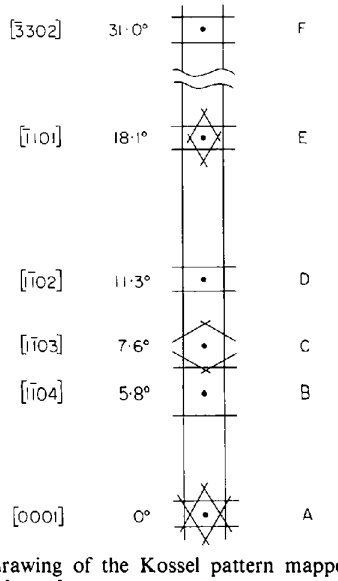

Fig. 1. Line drawing of the Kossel pattern mapped between the [$\bar{3}$302] and [0001] axes of GaS, following the main $11\bar{2}0$–$\bar{1}\bar{1}20$ reflexion lines. The spacings are drawn to a consistent scale (given by the convention of cylindrical projection for a narrow spherical section). The angles written beside each zone represent a rotation angle (°) from the [0001] zone.

internal mirror line (Fig. 3*b*, see also Fig. 5). *E* and *F* zones could be rejected as major zones of the space-group system by the following analysis. The appearance of extra reflexions between these zones indicated that the crystal would either have an orthorhombic space group with general extinction rules, $h + k + l = 2n$ (for *E* as the zero-layer zone) or with $h + k = 2n$; $k + l = 2n$ (for *F* as zero-layer zone). Neither of these classifications was consistent with the symmetry of the patterns. The lack of a horizontal mirror plane, *i.e.* one *normal* to the incident beam, in the structure at these settings (as evidenced by the lack of inversion symmetry in the central beam and satisfied *hkil* beams), combined with the identification, below, of a centre of symmetry in the structure, was convincing proof that we had not yet arrived at the principal axis.

Test for centre of symmetry

A test for a centre of symmetry can be carried out with advantage at a setting of low symmetry (Goodman, 1975). Consequently, a pair of patterns was taken about the zone *F*, satisfying the *hkil* and $\bar{h}\bar{k}\bar{i}\bar{l}$ reflexions. The results appear in Figs. 3(*c*) and 3(*d*). This zone axis was later identified as $[\bar{3}302]$ (Fig. 1) at an angle of 31° to the *c* axis, and the reflexion pair as $1\bar{1}03/\bar{1}1\bar{0}\bar{3}$. These patterns satisfy the condition for conjugate excitation, achieved by exchanging the positions of the 0000 and *hkil* discs between patterns. The 0000, *hkil* discs were chosen to have a common mirror line; the single mirror line of the pattern. However, they had no other symmetry. Therefore, it was easy to identify a translation between characteristic $hkil/\bar{h}\bar{k}\bar{i}\bar{l}$ conjugate patterns which is the positive indication of centrosymmetry. Typically, the 0000 discs show no interrelation: one has a striking resemblance to a cat face with open eyes; in the lower face the 'eyes' are closed. The *hkil* pair show a close one-to-one correspondence in geometric detail, thus confirming the existence of a structural centre of symmetry to high accuracy.

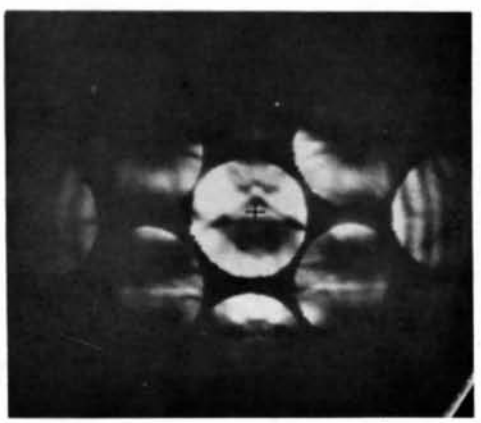

Fig. 2. The pseudo-hexagonal pattern from the $[\bar{1}101]$ zone axis (*E* of Fig. 1) located by an 18·1° rotation from [0001].

The crystal was next rotated in the reverse sense to the previous rotation about the original rotation axis. Rotations about this axis, $[11\bar{2}0]$, will retain the symmetries (of a parallel twofold axis and a vertical mirror plane perpendicular to the axis) already identified and allow one to look for additional symmetries. Rotation was carried out past *E* to the new zone *D*, shown in Fig. 4(*a*). This pattern again, including the zero-beam distribution, has only 1*m* symmetry, showing as before that we have no (central) horizontal mirror plane in this setting. The pair of conjugate first-order ($1\bar{1}01$ indexed) excitations of Figs. 4(*b*) and (*c*) shows two things: firstly, the confirmation of centrosymmetry by identification of fine detail, using the same test as in Fig. 2 and secondly, the lack of mirror-line symmetry of this detail internally shows that no new twofold axis has been found in this direction. The simpler patterns obtained compared with Fig. 2 show that we have weaker interactions at this zone. The fine detail in Figs. 4(*b*) and (*c*) arises largely from upper-layer interactions and was produced by tilting the incident beam slightly out of the mirror plane.

Further crystal rotation in the same direction took the setting past *C* to zone *B* (of Fig. 1). Now a four-beam pattern was taken, to test for the approach of a central horizontal mirror plane (the extra symmetry required for consistency). The corner beam encircled in this pattern (Fig. 5) (indexed $20\bar{2}1$) does not quite have an internal inversion centre, the upper diagonal branch of the crossing line being weaker than the lower branch; the result, however, indicates that the rotations are now in the correct direction for increasing symmetry.

At this stage of the experiment we had reached the end of the goniometer range in this direction (having traversed about 20° from the initial arbitrary setting). Therefore, the specimen support was removed and replaced in the goniometer head with an appropriate inclination to permit the experiment to continue. The identical crystal region was then relocated using the defocused-beam image. The next zone, *A*, was readily identified as the c^* axis from its high symmetry. Further analysis therefore involved exploration of this immediate region, as well as later further rotation to the mirror image of zones already identified at angles on the reverse side of the principal zone.

Identification of the [0001] zone in Fig. 6(*a*) allowed all the patterns to be indexed on the hexagonal system. Centrosymmetric space groups of the hexagonal system form two sets, namely numbers 175–176 and 191–194, where the number identification from *International Tables for X-ray Crystallography* (1965) is used for convenience. The former set, however, has no twofold axes and no vertical mirror planes, and is therefore excluded. The systematic absences which distinguish the four groups 191–194 are shown in Table 1.

Figs. 6(*b*), (*c*) and (*d*) show proof of the existence of twofold axes at intervals of 30° around the zone

(parallel to the $[1\bar{1}00]$ and $[11\bar{2}0]$ directions). This character occurs only in the sets 177–182 (non-centrosymmetric) and 191–194 of space groups. Here, this represents further confirmation that the identification 191–194 is correct; in another analysis, for instance one confined to the neighbourhood of the principal zone, this type of pattern can be essential to the analysis.

Test for space-group-forbidden reflexions

According to Table 1, space groups 192–193 must be ruled out, since the $h0\bar{h}l$ reflexions with $l = 2n + 1$ are not forbidden and are quite strong (see Fig. 3). Conditions for detecting space-group-forbidden reflexions have been laid out by Gjønnes & Moodie (1965) and, in the case where they arise from the action of vertical glide planes (as at present), require that the reflexions under test be examined in a particular way, namely, with the incident beam parallel to the glide plane in question. To test for the second condition, $hh\bar{2}\bar{h}l$ forbidden for $l = 2n + 1$, the crystal must be rotated about a $1\bar{1}00$-indexed axis. This has been done in Fig. 7. The reflexion $11\bar{2}1$, which has been encircled, shows a line of zero intensity through its central line of symmetry. In addition, the immediate vicinity of the reflexion is weak. This is a typical appearance for a space-group-forbidden reflexion under dynamic interaction and

Table 1. *Summary of the relative requirements of space groups* 191–194 *with regard to systematic absences*

Conditions: (1) $h0\bar{h}l$, $l = 2n$; (2) $hh\bar{2}\bar{h}l$, $l = 2n$.

Space-group number	Conditions
191	Neither
192	(1) & (2)
193	(1)
194	(2)

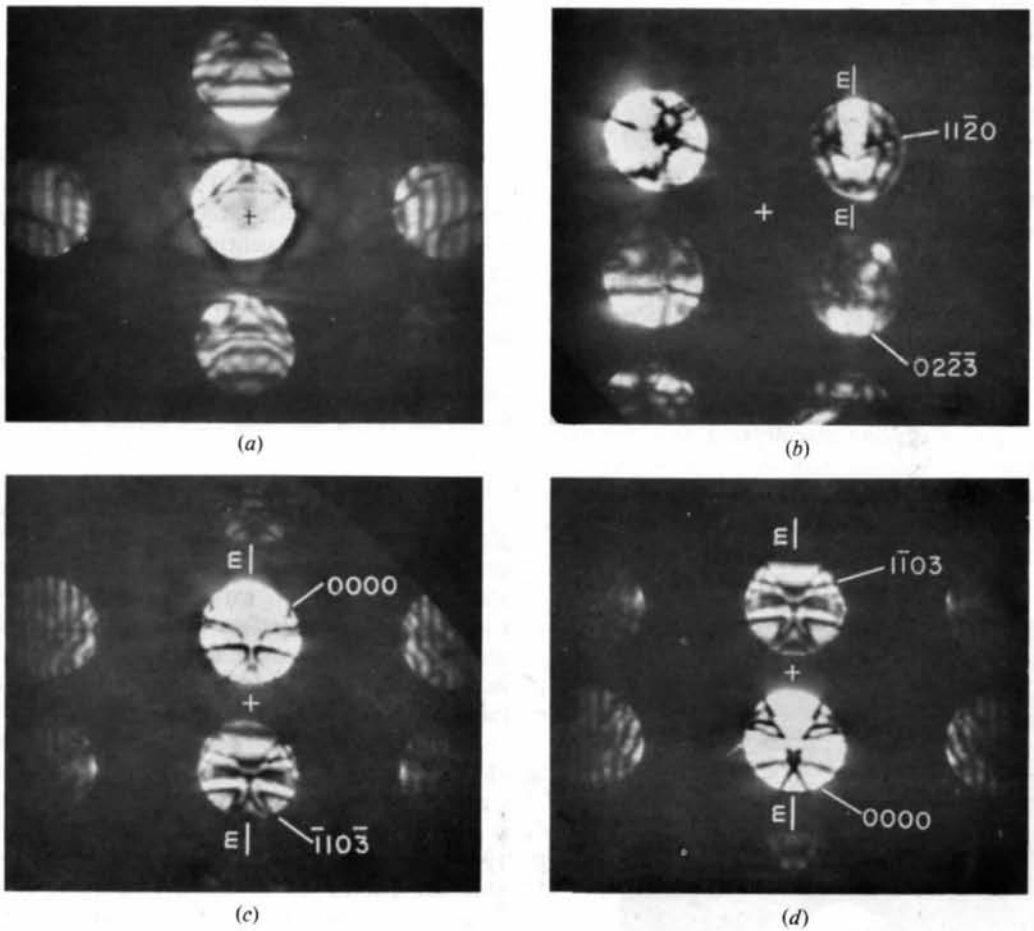

(*a*) (*b*) (*c*) (*d*)

Fig. 3. Data taken from the $[\bar{3}302]$ zone (F in Fig. 1). (*a*) Zone-axis setting. (*b*) Four-beam excitation, showing the mirror line in the $11\bar{2}0$ distribution. The mirror line indicates the existence in the structure of a twofold rotation axis parallel to the $[11\bar{2}0]$ direction (and perpendicular to the mirror line, drawn m–m). (*c*) and (*d*) These pictures show the conjugate excitation of the $\bar{1}10\bar{3}/1\bar{1}03$ reflexion pair. An almost perfect intensity-distribution identity is seen for the diffracted beams. The central mirror line of the whole pattern is indicated by the lines m–m in both bases. In all four pictures, the exact zone-axis position is indicated by a cross.

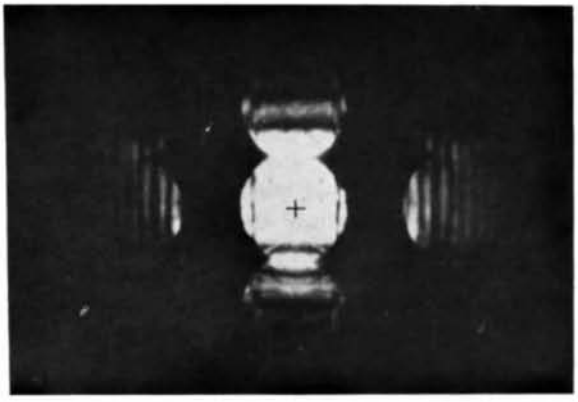

(*a*)

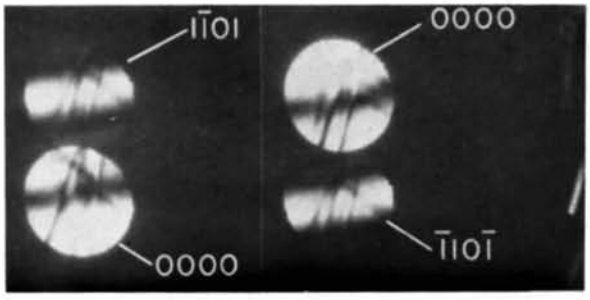

(*b*)

Fig. 4. Data from the vicinity of the $[1\bar{1}02]$ zone axis. (*a*) Zone-axis pattern. (*b*) $1\bar{1}01/\bar{1}10\bar{1}$ reflexions shown in conjugate excitations, to demonstrate a centre of symmetry in the structure. These patterns were taken at a small inclination to the $[1\bar{1}02]$ axis.

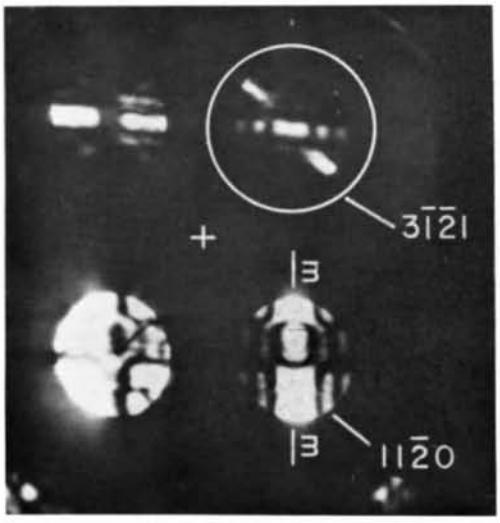

Fig. 5. Four-beam pattern taken about the $[1\bar{1}04]$ zone axis (marked by a cross). Note that (i) the $11\bar{2}0$ reflexion has a central mirror line, confirming the structural twofold axis, noted also from Fig. 4(*b*), and (ii) the $3\bar{1}\bar{2}1$ reflexion encircled has almost, but not quite perfect, inversion symmetry, the symmetry departure being observable in the diagonal crossing line.

confirms the existence of the above general condition for the space group, using the Gjønnes–Moodie rules. Therefore, space-group 194, or $P6_3/mmc$, is the correct space group for GaS.

Comment

With regard to the problem of identifying a principal axis, the general recommendation is to rotate the crystal around an axis suggested by the symmetry of a zone pattern and to look for a *maximization* of symmetry. It is often fairly simple to see if a particular rotation has led to an approach to higher symmetry. If this test is not made, a single low-symmetry zone pattern could lead to the wrong allocation of a lower symmetry to the whole structure. The other useful criterion (besides looking for a symmetry maximum) is one of internal consistency, *i.e.* between the systematic absences and the zone symmetries.

The space group of GaS could be established from the evidence of Figs. 3, 6 and 7, and a more compact description could be given. However, the additional patterns are useful in establishing the validity of the three-dimensional-interaction interpretation, given only in principle in earlier publications. The degree of upper-layer interaction (or alternatively the departure from the projection approximation) in this structure, with a *c* axis of 15·5 Å, is very evident, and can be examined in patterns taken away from the [0001] zone axis. The asymmetry introduced in these patterns arises from the inclination both of the unit cell and of the surface normals to the incident beam. The effect is very evident in Figs. 2 and 3 with inclinations of 18 and 31°, respectively, and is evident in Fig. 5 with an inclination of only 8°. The results here clearly demonstrate the utility of using the inclined-axis technique for identifying a centre of symmetry, especially in the presence of other symmetry elements.

The patterns in the above analysis were taken with 80 kV electrons, a crystal thickness of 780 Å, and a specimen temperature of approximately 173 K.

Space-group determination of $Cu_3As_2S_3I$

$Cu_3As_2S_3I$ was prepared by mixing CuI, Cu and As_2S_3 powders in the correct proportions, and heating them together in an evacuated glass ampoule for 48 h at 693 K. A homogeneous mass of red platelets was obtained. Initial examination by X-ray diffraction suggested that the crystals were hexagonal with the conditions $000l$, $l = 2n$, *i.e.* the intensity distribution was hexagonal about the *c* axis. The dimensions of the hexagonal cell were $a = 7{\cdot}16$ and $c = 41{\cdot}1$ Å. Alternatively, the crystals could be indexed in the orthorhombic system with cell dimensions $a = 7{\cdot}16$, $b = 12{\cdot}37$ and $c = 41{\cdot}1$ Å.

A crystal from the same sample was cleaved mechanically and placed into the cold stage of a modified Elmiskop 1 microscope (Dowell & Williams, 1976). Convergent-beam patterns taken at the principal axis immediately showed an orthorhombic rather than a hexagonal symmetry of intensities. The pseudo-hexagonal symmetry, which is difficult to see in the convergent beam patterns, is obvious in the corresponding focused point pattern (inset in Fig. 8), which allows us to index all the reflexions in agreement with the X-ray data. The Kossel (wide-angle) pattern which is taken as a preliminary (Fig. 8*a*), however, already shows rectangular symmetry. The corresponding convergent-beam pattern at the zone axis (Fig. 8*b*) clearly shows this, with approximately $2mm$ symmetry in the zero layer ($l = 0$), but only $1m$ symmetry in the upper layer ($l = 1$). The conditions now required, in addition to those found by X-ray diffraction, are $h + k = 2n$, and rectangular coordinates. The higher symmetry observed for $l = 0$ could indicate an approach to the 'projection approximation' in this layer, and hence indicate a projection symmetry of Cmm for [0001].

Two more patterns were taken to examine this point more closely, with symmetrical excitation about the $0k0$ and $h00$ lines of the zone-axis pattern, respectively. In the former case (Fig. 9*c*), the pattern shows a

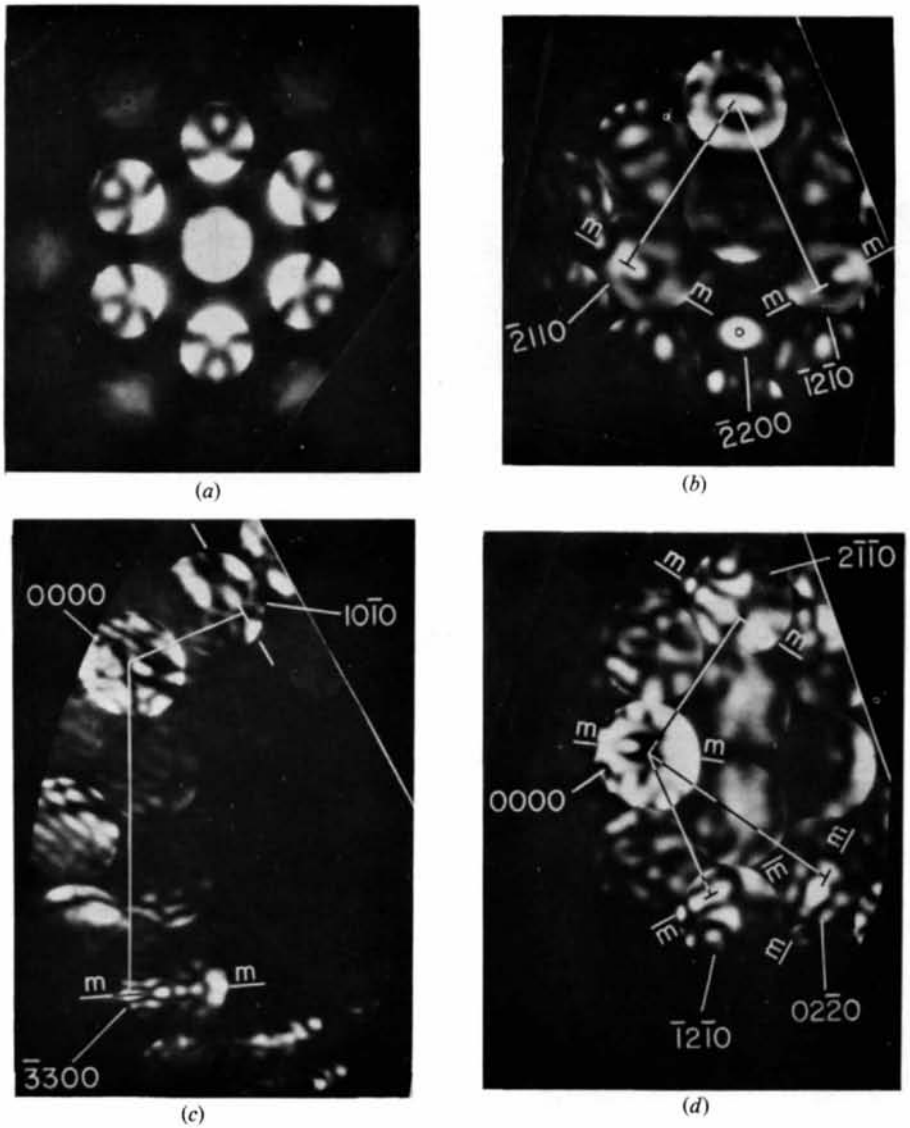

Fig. 6. Data taken from the vicinity of the [0001] zone axis. (*a*) The exact [0001] zone-axis pattern, showing the sixfold rotation symmetry. (*b*) Symmetrical excitation of the $\bar{2}200$ reflexion showing: (i) an inversion centre in the $\bar{2}200$ reflexion; (ii) mirror lines (m–m) in the $\bar{2}110$ and $\bar{1}2\bar{1}0$ reflexions, at a 60° interval, and also a mirror line in the 0000 disc (not indicated, but bisecting this angle). (*c*) Exact excitation of $10\bar{1}0$ and $\bar{3}300$ reflexions, showing respective mirror lines m–m at a 120° interval. (*d*) Symmetrical excitation of $2\bar{1}\bar{1}0$ and $\bar{1}2\bar{1}0$ reflexions, and incidental excitation of the $02\bar{2}0$ reflexion. Mirror lines are shown in these reflexions, showing both a 30 and a 60° interval.

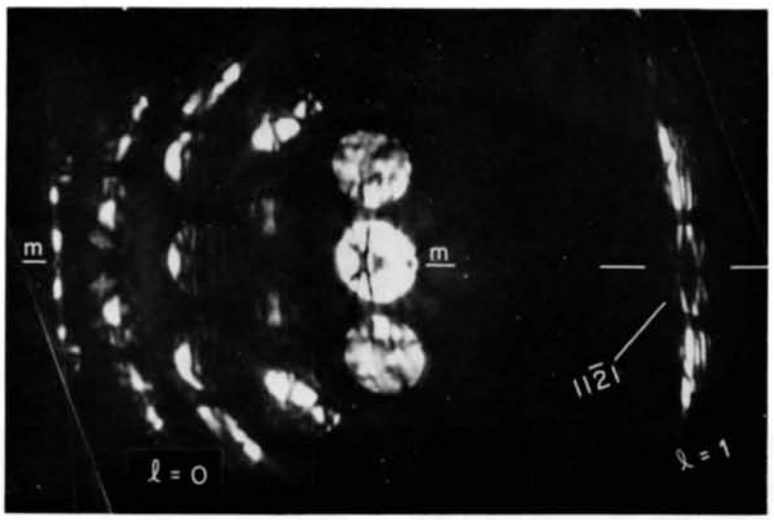

Fig. 7. Exact symmetrical excitation of the 11$\bar{2}$1 reflexion. This setting is obtained by a rotation from the [0001] axis which is perpendicular to that used for the series of rotations depicted in Fig. 1. The typical Gjønnes–Moodie extinction line is shown, lying along the general mirror line of the whole pattern.

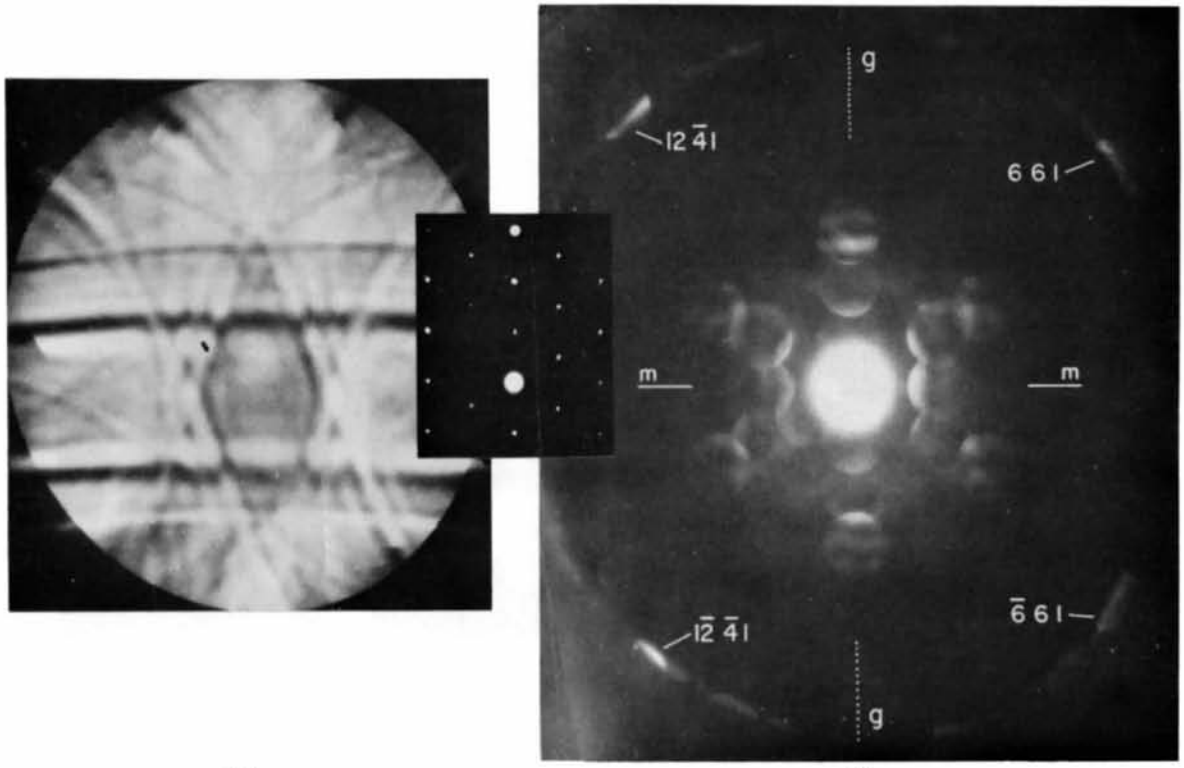

(*a*) (*b*)

Fig. 8. Patterns taken at the principal, pseudo-hexagonal zone axis of $Cu_3As_2S_3I$. (*a*) Wide-angle illumination, giving the electron Kossel pattern of the zone. (*b*) Convergent-beam pattern showing a rectangular pattern symmetry. The inset shows a focused-beam point pattern from the same setting showing the apparent hexagonality, and allowing the patterns to be indexed readily in agreement with the X-ray data. Two regions are visible in the convergent-beam pattern: (i) the zero-layer region shows an approximate 2*mm* symmetry; (ii) the first upper-layer (outer ring) reflexions show only one mirror line or 1*m* symmetry: the 12,$\bar{4}$,1/$\bar{1}\bar{2}$,$\bar{4}$,1 reflexions are mirrored across *m*–*m*, but not across the vertical line *g* ... *g*.

complete mirror symmetry about the $0k0$ line. In the latter case (Fig. 9*a*), the diffraction pattern shows a fairly perfect mirror symmetry about the $h00$ line *except* in the zero beam 000. This beam shows an internal asymmetry about the $h00$ line. This evidence is consistent with the structure having only one set of vertical mirror planes, parallel to $[0k0]$, the second partial mirror symmetry being generated by the projection of a set of glide planes having a z translational component (or a set of twofold axes; Goodman, 1975). The information obtained so far, including the X-ray condition, $000l$, $l = 2n$, is consistent with only two space groups, namely No. 36 (non-centrosymmetric) and No. 63 (centrosymmetric) of the orthorhombic system [*International Tables for X-ray Crystallography* (1965) nomenclature]. Further information can be extracted from the pattern of Fig. 9(*a*) as follows:

(1) The asymmetry in the 000 beam about the vertical (dotted) line of the figure means, when the horizontal mirror lines are taken into account (full lines in Fig. 9*c*), that the complete 000 distribution will have only a $1m$ symmetry and will lack a centre of inversion. This means, according to the interpretative rules for dynamic interaction, that the crystal as a whole has no exact central mirror plane perpendicular to [001].

(2) The excited 12,0,0 reflexion appears to have

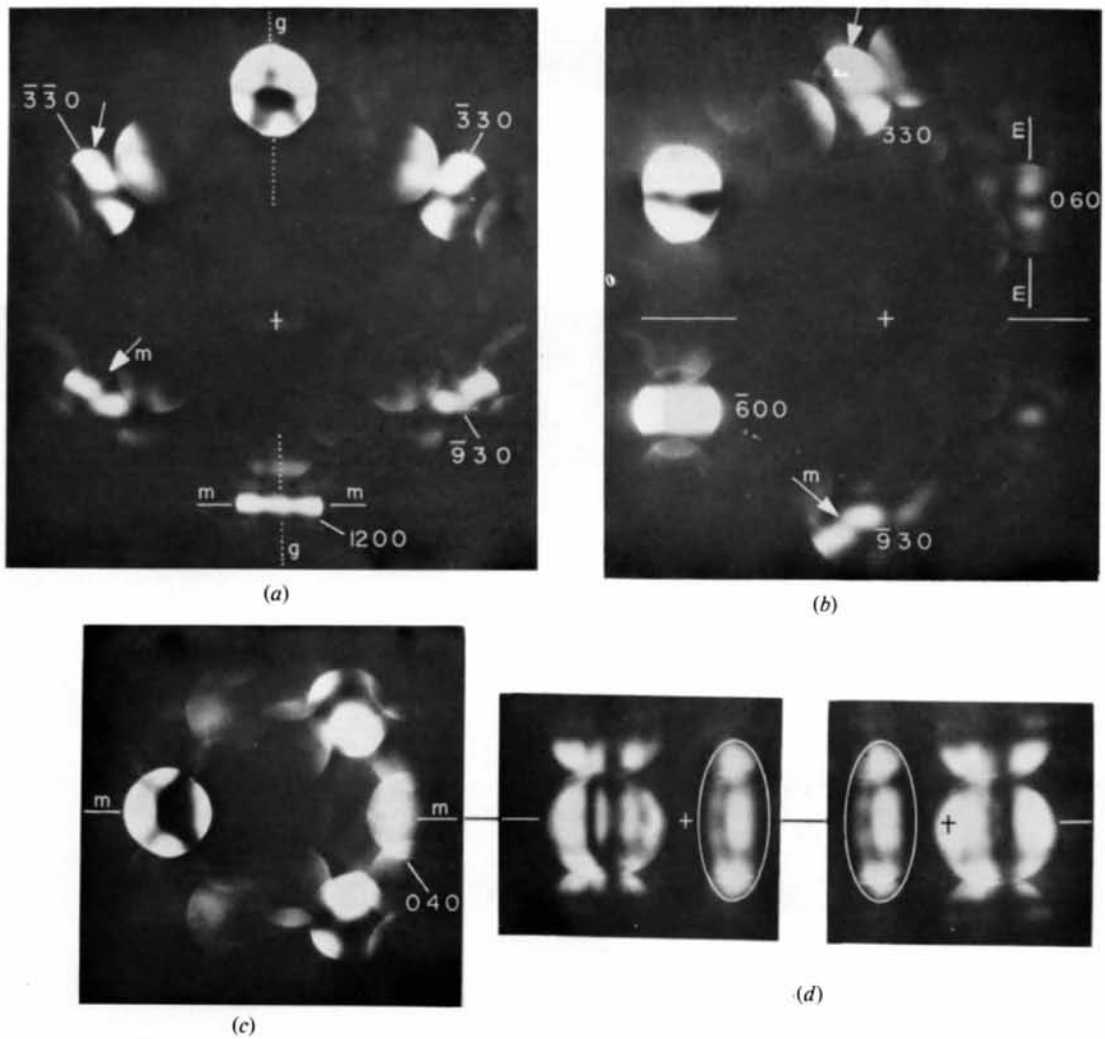

Fig. 9. (*a–c*) Patterns taken around the [001] zone axis. (*a*) Exact symmetrical excitation of the 12,0,0 reflexion showing an approximate mirror line through the whole pattern, with the exception of the 000 disc. The 000 disc shows a departure from mirror symmetry about the vertical $g \ldots g$ line, typical of the action of a structural glide plane having a 'z' translational component. Also shown is a mirror line through the 12,0,0 reflexion. (*b*) Conjugate excitation, with respect to (*a*), of the 330 reflexion. Conjugate pairs are indicated by arrows, conjugate mirror pairs by subscripted '*m*' arrows (see text). Also shown is a mirror line through the exactly excited 060 reflexion. (*c*) Exact symmetrical excitation of the 040 reflexion, showing an exact mirror-line symmetry through the whole pattern, about the $0k0$ line (indicated by the line m–m). (*d*) Conjugate excitation of the $2\bar{2}01/\bar{2}20\bar{1}$ reflexion pair at an inclined setting, showing an intensity identity for the diffracted beams.

internal mirror-line symmetry; this would imply that the crystal has a twofold rotation axis parallel to [h00].

(3) A third pattern was taken (Fig. 9b) by placing the incident beam aperture over the third-order position (indexed $\bar{3}\bar{3}0$) of the previous pattern (Fig. 9a), thus exciting the $33\bar{0}$ reflexion in conjugate relationship to the previous $\bar{3}\bar{3}0$ excitation, *i.e.* we have set up the conjugate excitations required to test for centrosymmetry. Also, taking into account the mirror line through [0k0], the excitation of the $9\bar{3}0$ reflexion in the pattern (Fig. 9b) corresponds to the *mirrored* conjugate excitation of the $\bar{9}\bar{3}0$ reflexion in the previous (Fig. 9a) pattern. [To see this relationship, reflect the pattern of Fig. 9(b) about the horizontal line indicated on the figure; we then obtain the pattern equivalent to that obtained by interchanging the incident 000 beam with the $\bar{9}\bar{3}0$ beam in Fig. 9(a).] If the crystal were centrosymmetric, these conjugate pairs would show a translational intensity relationship between the $hkl/\bar{h}\bar{k}\bar{l}$ pairs (arrowed in the two figures). This relationship is apparent, but is not accurately observable.

Test for centre of symmetry

The above observations illustrate some of the difficulties which can be encountered in applying the centrosymmetry test. The difficulties here are twofold: (a) a combination of spherical aberration and crystal curvature acts to distort the intensity distributions when the incident aperture is shifted off-axis; (b) with this particular structure a limit to the usable crystal thickness, set by absorption, an appreciable temperature effect, and a crowded diffraction pattern all act to limit the amount of information which can be obtained in a diffraction disc.

These difficulties can be partly mitigated by rotating the crystal, both to move away from the zone pattern and to obtain a tilted illumination. A rotation of a few degrees was made about the 'a' axis, so as to excite a 02l reflexion, while at the same time retaining the central mirror line in the pattern (the incident beam is still parallel to the mirror planes of the structure). This inclination to the surface normal and also to the 'c' axis was now sufficient to give a distinctive asymmetry to the 02l intensity pattern (Fig. 9d). When the conjugate 02l pattern was taken (also shown in Fig. 9d), the translational relationship was easily identified. By retaining the symmetry line of the pattern the identification was easier because now the overlapping trio of reflexions 22l–02l–$\bar{2}$2l, could be used as a single distribution in the test. To avoid lens distortion effects, the conjugate pair was taken symmetrically about the instrumental axis.*

The observations of Fig. 9 show that the crystal is centrosymmetric and belongs to space group No. 63 (*Cmcm*) rather than to No. 36 ($Cmc2_1$). This would also be the conclusion from the identification of twofold axes from Figs. 9(a) and (b). However, in this case the centrosymmetric test was the more definite.

Comment

The patterns from $Cu_3As_2S_3I$ were not of such good quality as those from GaS. This was partly due to the more complicated structure having a higher temperature factor and a greater ratio of absorption to elastic scattering, but also to the fact that less time was given to this analysis. Approximately 21 d was given to collecting data for GaS as against 3 d for the $Cu_3As_2S_3I$ data. The symmetry of the latter compound was uniquely determined, nevertheless, because it was feasible to use the data together with X-ray single-crystal data. The hexagonal symmetry in the latter data was finally attributed to multiple twinning around the 'c' axis, *i.e.* 60° twinning or 'trilling'. It would have been possible of course to get all the necessary 'c' axis information from electron diffraction with a little more work, but the X-ray data was certainly required in order to obtain accurate cell dimensions. In other words, when both techniques are available, the work is much more efficient because different parameters are measured with greater sensitivity and accuracy in each case.

The patterns presented here were taken with both 80 and 100 kV electrons and with a specimen temperature of approximately 173 K.

Conclusions

These two studies of inorganic materials clearly show the applicability of systematic space-group identification procedures previously outlined only in principle. This applies particularly to the procedure for direct identification of a centre of symmetry, and hence to distinguishing between centrosymmetric and non-centrosymmetric space groups. This appears to be the single most urgent addition to normal X-ray procedures. If we can take the example of GaS as typical in any way, the present method of electron diffraction appears superior diagnostically to the spectroscopic alternative of higher-harmonic generation which, on its own, would have indicated non-centrosymmetry (see for example van der Ziel, Meixner & Kasper, 1973).

* When these last pairs of pictures were taken an instrumental fault had already developed. A fault in the high-tension cable led to a double source, which can be detected in Fig. 9(d). This fault fortunately does not obscure the test.

References

BASINSKY, Z. S., DOVE, D. B. & MOOSER, E. (1961). *Helv. Phys. Acta*, **34**, 373–378.

DOUGHERTY, J. P. & KURTZ, S. K. (1976). *J. Appl. Cryst.* **9**, 145–158.
DOWELL, W. C. T. & WILLIAMS, D. (1976). *Ultramicroscopy*, **2**, 43–48.
GJØNNES, J. & MOODIE, A. F. (1965). *Acta Cryst.* **19**, 65–67.
GOODMAN, P. (1975). *Acta Cryst.* A**31**, 804–810.
HAHN, H. & FRANK, G. (1955). *Z. Anorg. Chem.* **278**, 340–348.
International Tables for X-ray Crystallography (1965). Vol. I. Birmingham: Kynoch Press.
TANAKA, M. (1978). Private communication.
ZIEL, J. P. VAN DER, MEIXNER, A. F. & KASPER, H. M. (1973). *Solid State Commun.* **12**, 1213–1215.

Acta Cryst. (1980). A**36**, 228–237

Short-Range Order and Superstructures of Ternary Oxides AMO_2, A_2MO_3 and A_5MO_6 of Monovalent A and Multivalent M Metals Related to the NaCl Structure

BY J. HAUCK

Institut für Festkörperforschung der KFA Jülich, D-5170 Jülich, Federal Republic of Germany

(*Received* 6 *June* 1979; *accepted* 20 *July* 1979)

Abstract

Ternary oxides AMO_2, A_2MO_3 and A_5MO_6 with monovalent A and tri-, tetra- or hepta-valent M metals can exhibit order/disorder transitions with about 20 superstructures of the NaCl lattice. Some structures can be related to AM, A_2M and A_5M alloys with a larger distortion of the lattice due to stronger interactions between metal atoms. In ternary oxides about 30 short-range order configurations are selected for the first, second and third shell of metal atoms in applying Pauling's electrovalence rule. Stable configurations are characterized by the strength of Coulomb interactions and by a high point symmetry of the M atoms. Mainly disordered ternary oxides can vary stoichiometrically with a frequent occurrence of vacancies or with partial occupation of tetrahedral interstices by A atoms.

I. Introduction

Many ternary oxides with the composition AMO_2, A_2MO_3 and A_5MO_6 of monovalent A and tri-, tetra- or hepta-valent M metals exhibit crystal structures closely related to the NaCl structure. The A and M metal atoms are distributed randomly or are in an ordered superstructure occupying Na positions, while O atoms are on the Cl positions. This might be due to the stability of the NaCl structure for octahedrally coordinated A and M atoms at 1:1 metal/oxygen ratio and the Coulomb interactions in ternary oxides. Pauling's electrovalence rule is strictly held only for these particular compositions. The sum of the electrovalencies z/n (z = charge, n = coordination number) of the six nearest A and M neighbours of each O atom should be equal to the charge of ionic oxygen:

$$\tfrac{1}{2}A^{+1}M^{+3}O_2 = A^{+1}_{3/6}M^{+3}_{3/6}O,\ \sum z/n = 3\times\tfrac{1}{6} + 3\times\tfrac{3}{6} = 2;$$

$$\tfrac{1}{3}A^{+1}_2M^{+4}O_3 = A^{+1}_{4/6}M^{+4}_{2/6}O,\ \sum z/n = 4\times\tfrac{1}{6} + 2\times\tfrac{4}{6} = 2;$$

$$\tfrac{1}{6}A^{+1}_5M^{+7}O_6 = A^{+1}_{5/6}M^{+7}_{1/6}O,\ \sum z/n = 5\times\tfrac{1}{6} + 1\times\tfrac{7}{6} = 2.$$

The electrovalency of oxygen is compensated only when it has either three trivalent, two tetravalent or one heptavalent besides the monovalent metal atoms as nearest neighbours.

II. Short-range order models

Short-range order has been investigated for f.c.c. alloys (Tanner & Leamy, 1974) and can be compared with the ternary oxides of this investigation. In many cases alloys of metals A and M with composition AM, A_2M or A_5M show the same or closely related superstructures as the metal atoms of AMO_2, A_2MO_3 or A_5MO_6 ternary oxides. The short-range order configurations of the disordered alloys may usually be related to the ordered superstructures (Clapp, 1971). Because of the large variety of the short-range order configurations and the weak interactions between the metal atoms, the nearest neighbours only are considered for short-range ordering of alloys. In this investigation short-range order configurations favoured by somewhat stronger Coulomb interactions in ternary oxides are selected. The location of the highly charged M atoms in the first three shells around each M atom with the translational vectors $\mathbf{T}_1 = (a/2\ a/2\ 0)$, $\mathbf{T}_2 = (a\ 0\ 0)$ and $\mathbf{T}_3 = (a\ a/2\ a/2)$ are considered. According to Pauling's rule the variety of short-range order con-

0567-7394/80/020228-10$01.00